*J. Fluid Mech.* (2004), *vol.* 500, *pp.* 55–64.  
DOI: 10.1017/S0022112003007225 Printed in the United Kingdom

# A continuum and molecular dynamics hybrid method for micro- and nano-fluid flow

By X. B. NIE[1], S. Y. CHEN[1,2], W.N. E[3,2] AND M. O. ROBBINS[4,1]

[1]Department of Mechanical Engineering, The Johns Hopkins University, Baltimore, MD 21218, USA

[2]CCSE and LTCS, Peking University, Beijing, China

[3]Mathematics Department, Princeton University, Princeton, NJ 08544, USA

[4]Department of Physics and Astronomy, The Johns Hopkins University, Baltimore, MD 21218, USA

(Received 8 July 2003 and in revised form 30 October 2003)

A hybrid multiscale method is developed for simulating micro- and nano-scale fluid flows. The continuum Navier–Stokes equation is used in one flow region and atomistic molecular dynamics in another. The spatial coupling between continuum equations and molecular dynamics is achieved through constrained dynamics in an overlap region. The proposed multiscale method is used to simulate sudden-start Couette flow and channel flow with nano-scale rough walls, showing quantitative agreement with results from analytical solutions and full molecular dynamics simulations for different parameter regimes. Potential applications of the proposed multiscale method are discussed.

## 1. Introduction

Continuity is the most fundamental assumption in macroscopic fluid mechanics which is governed by the Navier–Stokes (NS) equations (see, for example, Batchelor 1967). This assumption breaks down as the spatial scale of flows approaches the molecular mean free path (Ho & Tai 1998). The discreteness of matter is important in a growing number of applications, such as micro-electro-mechanical systems (MEMS), that involve flow in micrometer- and nanometer-scale channels. Continuum approaches also fail to describe macroscopic flows where the continuum equations have essential singularities, as in the moving contact-line problem (Huh & Scriven 1971; Dussan 1979; Dussan & Dave 1986).

Atomistic descriptions, such as molecular dynamics (MD) simulations, are capable of modeling nano-fluid and singular flows (Koplik & Banavar 1995*a*, *b*; Thompson & Troian 1997; Koplik, Banavar & Willemsen 1988; Thompson & Robbins 1989). However, it is unrealistic to use full MD simulations to study flows at micro-scales because of memory and computational time limitations. Moreover, in most cases the breakdown of the continuum description is confined to limited domains, such as fluid–fluid or fluid–solid interfaces. Hence it is desirable to develop hybrid methods that combine continuum fluid dynamics and molecular dynamics, using the most efficient description in each region of space.

Figure 1 shows a general schematic of the geometry of a hybrid scheme. Continuum equations are solved in regions that are homogeneous and have small velocity gradients (shaded region). An atomistic description, for example MD simulation, is used at interfaces or where gradients are large (region with discrete circles). The

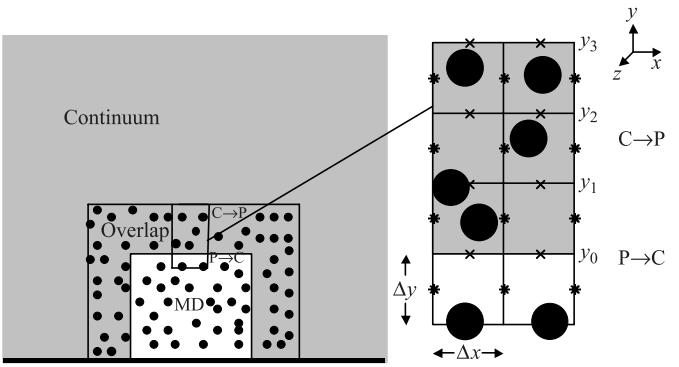


FIGURE 1. Schematic of the hybrid method. The continuum description is used in the shadowed region and the atomistic description is used in the dotted region. In C → P, continuum solutions provide boundary conditions for MD simulations and in P → C atomistic solutions provide boundary conditions for continuum simulations.

major technical difficulty in constructing such methods lies in coupling these very different descriptions of fluids at the MD–continuum interface. The two descriptions in the overlap region are coupled and must be consistent, i.e. the physical quantities, including density, momentum and energy, and their fluxes, must be continuous. The boundary conditions needed for the continuum equations can be straightforwardly obtained by averaging the corresponding quantities from the particle description over the local region and over time. However, the reverse problem, generating microscopic particle configurations from known macroscopic quantities such as density, momentum and energy, is non-trivial and must necessarily be non-unique. The problem is magnified when there is flux of particles between continuum and discrete regions. In general, there is also a time coupling issue since the integration time step for the continuum Navier–Stokes equations is normally several orders of magnitude larger than that in the MD region.

Several coupling schemes have been developed. O'Connell & Thompson (1995) noted that it was important to have a finite overlap region to avoid sharp density oscillations and allow the two solutions to relax before they are coupled together. They used a relaxation method to force the average MD velocity in a region to follow the continuum solution. This introduces an arbitrary relaxation rate, but the more important limitation of their approach is that it does not include mass flux at the MD–continuum interface. This limited the geometries they could consider, but their approach successfully reproduced a set of one-dimensional flows.

Hadjiconstantinou & Patera (1997) developed a Maxwell Demon method for simulating incompressible flow. Particle velocities are drawn from a Maxwellian distribution with mean and standard deviation determined by the local continuum velocity and temperature. A particle reservoir is used to conserve mass flux across the MD–continuum interface. Periodic boundary conditions are applied to the MD simulation domain, including the reservoir. This prevents particles from drifting away, but may introduce spurious correlations, and limits the geometry of the MD region. Schwarz iteration is used to make the MD and continuum descriptions consistent. They simulated a steady channel flow with an obstacle (Hadjiconstantinou & Patera 1997) and the moving contact-line problem (Hadjiconstantinou 1999). The results are fairly consistent with full continuum or full MD simulations.

More recently Flekkoy, Wagner & Feder (2000) presented a new hybrid method for isothermal, compressible flow. Their scheme is based on continuity of mass and momentum fluxes across the MD–continuum interface. Steady Couette flow and steady Poiseuille flow were simulated to demonstrate the method. However, our tests of this algorithm indicate that it may become unstable in more complicated geometries, including the case of channel flow past a rough wall shown in figure 3.

In this paper we introduce a robust hybrid method that builds on these previous works. The continuum solution is obtained by numerically integrating the Navier–Stokes equations with boundary conditions that include information from the MD solution at P → C in figure 1. The MD equations are integrated with a much smaller time step, and the MD boundary conditions at C → P are obtained using 'constrained dynamics'. The MD equations in the interface region are modified to constrain the mean local particle velocity to equal the instantaneous continuum velocity, rather than relaxing to it over some time scale (O'Connell & Thompson 1995). The approach is tested against low-dimensional flows used in previous work, and in two-dimensional flows where there is flux across the MD–continuum interface.

## 2. Method

We begin by describing the pure continuum and MD simulations implemented in this paper. In the MD simulation, the molecular interaction potential is given by a shifted Lennard–Jones potential

$$V^{LJ}(r) = 4\epsilon\left[\left(\frac{\sigma}{r}\right)^{12} - \left(\frac{\sigma}{r}\right)^{6} - \left(\frac{\sigma}{r_c}\right)^{12} + \left(\frac{\sigma}{r_c}\right)^{6}\right]. \tag{2.1}$$

Here $\epsilon$ is the characteristic binding energy and $\sigma$ is the characteristic length, representing the molecular diameter. The interaction is set to zero when molecules are separated by more than the cut-off length $r_c = 2.2\sigma$. Molecules have mass $m$ and the mass density is set to $\rho = 0.81m\sigma^{-3}$.

The equations of motion are integrated using the Verlet scheme with time step $\Delta t_{MD} = 0.005\tau$, where $\tau \equiv (m\sigma^2/\epsilon)^{1/2}$ is the characteristic time of the Lennard–Jones potential. A Langevin thermostat with damping rate $\tau^{-1}$ is used to maintain a constant temperature of $1.1\epsilon/k_B$, where $k_B$ is Boltzmann's constant (Grest & Kremer 1986). The thermostat is only applied in the $z$-direction, since it is always normal to the mean velocity in the two-dimensional flows considered here. In more general geometries, or to include heat flux, one may apply the thermostat only in the middle of the overlap region, and only to the deviation from the mean local flow. At the above temperature and density, the molecules form a Lennard–Jones liquid with dynamic viscosity $\mu = 2.14\epsilon\tau\sigma^{-3}$ (O'Connell & Thompson 1995). This viscosity is used in the continuum equations.

The three-dimensional Navier–Stokes equations and the continuity equation in the continuum region are written as

$$\partial_t \boldsymbol{u} + \boldsymbol{u}\cdot\nabla\boldsymbol{u} = -\frac{1}{\rho}\nabla p + \nu\nabla^2\boldsymbol{u}, \tag{2.2}$$

$$\nabla\cdot\boldsymbol{u} = 0, \tag{2.3}$$

where $\boldsymbol{u}$ is the fluid velocity, $p$ is the pressure and $\nu = \mu/\rho$ is the kinematic viscosity. The above equations are solved numerically using the projection method. Space is discretized with mesh sizes $\Delta x = 5.21\sigma$, $\Delta y = 5.21\sigma$, and $\Delta z = 4.82\sigma$ in the

corresponding directions. For the two-dimensional flows considered here, there is no flow in the $z$-direction and periodic boundary conditions with period $\Delta z$ are applied to the MD simulations. The grid is illustrated in the enlargement of the overlap region shown at the right of figure 1. A staggered grid is used (see, for example, Peyret & Taylor 1983) with pressures defined at the centre of the cell and velocities in the middle of the sides of the cell. The $x$- and $y$-components of the velocity are defined at points indicated by asterisks and crosses, respectively. For accurate numerical integration of the continuum equations the time step $\Delta t_{FD}$ must be much smaller than the characteristic time of flows on the scale of the grid $\rho \Delta x \Delta y/\mu \sim 10\tau$. The continuum time step must also be larger than the velocity auto-correlation time $t_{vv}$ in order to minimize the thermal noise introduced by the boundary conditions. The two requirements place a lower limit on the cell size that is close to the choice used here. For the situations considered below, $t_{vv} \sim 0.14\tau$ (O'Connell & Thompson 1995), and we use $\Delta t_{FD} = 50\Delta t_{MD} = 0.25\tau$.

In the portion of the overlap region shown in figure 1, the lower boundary of the continuum cells is at $y = y_0$. The MD solution provides values of the $y$-component of the velocity at the crosses along $y = y_0$ and values of the $x$-component of the velocity at the asterisks along $y = y_0 - \Delta y/2$. These values are obtained by averaging the velocities of all MD particles within a volume of dimensions $\Delta x \times \Delta y \times \Delta z$ that is centred on the point of interest. The average is also performed over a time interval $\Delta t_{FD} = 0.25\tau$ that is centred on the time for the continuum equations. This means that information from the continuum simulation is only available for times $\Delta t_{FD}/2$ earlier than the current MD time. Note that smaller averaging regions and times would introduce more thermal noise into the continuum solution, and that the continuum velocities are already coarse-grained on these length and time scales.

The continuum and discrete descriptions propagate independently from $y_0$ to the height where the continuum solution provides boundary conditions for the MD solution. In future implementations, this region could be used for thermostatting or matching heat fluxes from the continuum and discrete solutions. However, in this work we minimized the width of the overlap region by applying the boundary condition at the second layer of cells, which lies between $y_1$ and $y_2$ in figure 1.

The average continuum velocity $\boldsymbol{u}_J$ in each cell $J$ is obtained by averaging the $x$- and $y$-velocities on the bounding edges. Continuity of the mean velocity requires that the averaged particle velocity in this cell is equal to $\boldsymbol{u}_J$:

$$\frac{1}{N_J}\sum_i \boldsymbol{v}_i = \boldsymbol{u}_J(t), \tag{2.4}$$

where $N_J$ is the number of particles in cell $J$. Taking a Lagrangian derivative of the above equation, we have $(1/N_J)\sum_i \ddot{\boldsymbol{x}}_i = \mathrm{D}\boldsymbol{u}_J(t)/\mathrm{D}t$. This constraint requires modification of the usual MD equations of motion: $\ddot{\boldsymbol{x}}_i = \boldsymbol{F}_i/m$, where $\boldsymbol{F}_i = (-\partial/\partial \boldsymbol{x}_i)\sum_{j\neq i} V^{LJ}(r_{ij})$. A general solution of the constraint equation can be written as

$$\ddot{\boldsymbol{x}}_i = \frac{\mathrm{D}\boldsymbol{u}_J(t)}{\mathrm{D}t} + \zeta_i, \tag{2.5}$$

where $\zeta_i$ is a variable whose sum over the cell is constrained: $\sum_i \zeta_i = 0$. To determine the optimum $\zeta_i$ we find the extremum of the time integral of the Lagrangian for the particles subject to the non-holonomic constraint of (2.4). Following standard

derivations (e.g. Saletan & Cromer 1971) one finds

$$\zeta_i = \frac{\boldsymbol{F}_i}{m} - \frac{1}{N_J m}\sum_{i=1}^{N_J} \boldsymbol{F}_i$$

which gives the following modified equation for the $i$th particle:

$$\ddot{\boldsymbol{x}}_i = \frac{\boldsymbol{F}_i}{m} - \frac{1}{N_J m}\sum_{i=1}^{N_J} \boldsymbol{F}_i + \frac{\mathrm{D}\boldsymbol{u}_J(t)}{\mathrm{D}t}. \tag{2.6}$$

In the simulation, (2.6) is discretized as

$$\frac{x(t+\Delta t_{MD}) - 2x(t) + x(t-\Delta t_{MD})}{\Delta t_{MD}^2} = \frac{\boldsymbol{F}_i}{m} - \frac{1}{N_J}\sum_{i=1}^{N_J}\frac{\boldsymbol{F}_i}{m} - \frac{1}{\Delta t_{MD}}\left(\frac{1}{N_J}\sum_{i=1}^{N_J}\dot{\boldsymbol{x}}(t)_i - \boldsymbol{u}_J(t+\Delta t_{MD})\right). \tag{2.7}$$

It can be proven that (2.7) is consistent with (2.4) and (2.6) to first order in $\Delta t_{MD}$. As mentioned above, the boundary conditions for the continuum equations are only known for a time $\sim\Delta t_{FD}/2$ earlier than the MD time. Thus $\boldsymbol{u}_J(t+\Delta t_{MD})$ is extrapolated from the continuum fluid velocity at the two nearest time steps.

O'Connell & Thompson (1995) used an equation similar to (2.6), but the final two terms on the right were multiplied by a number $\xi \ll 1$. This combined term then acts like a force driving the solution toward the constraint after a time of order $\Delta t_{MD}/\xi$. O'Connell & Thompson argued that this delay prevented the constraint from cancelling intrinsic thermal fluctuations on time scales less than $t_{vv}$. However, an undesirable consequence is that the particle velocities will always lag the continuum solution in an accelerating flow. O'Connell & Thompson found that large errors were introduced when they tried to increase $\xi$ toward unity. This may be because their algorithm used the same time step for the MD and continuum equations or because they used a different numerical scheme to integrate the continuum equations.

To prevent molecules from freely drifting away from the MD simulation domain, an external force is applied to particles between $y_2$ and $y_3$:

$$F_y = -\alpha p_0 \sigma \frac{(y-y_2)}{1-(y-y_2)/(y_3-y_2)}. \tag{2.8}$$

Here $p_0$ is the average pressure in the MD region, and $\alpha$ is a constant of order one. In the following we use $y_3 - y_2 = \Delta y$ and $\alpha = 1$, but the hybrid solution is not sensitive to factor of 2 changes in either parameter. The key constraints are that $F_y$ confine particles while minimizing density oscillations (O'Connell & Thompson 1995). The value of $y_3 - y_2$ must also be big enough to allow new particles to be introduced. The above constrained dynamics algorithm is used to match the mean velocity in the $x$-direction to the continuum solution for $y_2 < y < y_3$. The $y$-component of particle velocities is coupled to the heat bath for $y_2 < y < y_3$ to prevent overheating by the action of $F_y$.

To simulate mass flux across the MD–continuum interface, we change the number of particles in each cell by the net flux in an interval $\Delta t_{FD}$,

$$n' = -A\rho u_y \Delta t_{FD}/m, \tag{2.9}$$

where $A$ is the area of the cell perpendicular to the interface. If $n'$ is negative, the $n'$ particles closest to $y_3$ are removed. If $n'$ is positive, particles are inserted at regular

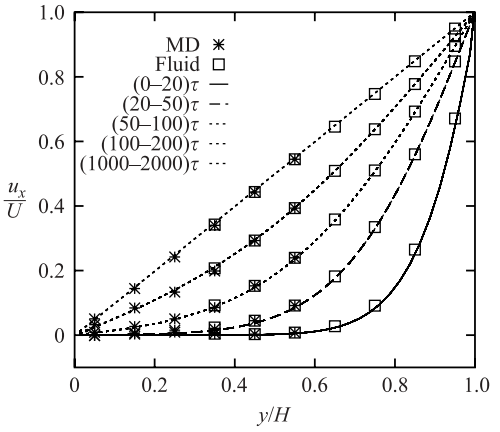


FIGURE 2. Velocity profiles at different times in sudden-start Couette flow. Lines show the solution of the Navier–Stokes equations averaged over the indicated time intervals. Hybrid results in the MD and continuum regions are shown by asterisks and squares, respectively. Hybrid results were averaged over ten independent runs to reduce thermal fluctuations.

intervals over the following $\Delta t_{FD}$ at positions near $y_3$ and randomly distributed along the interface. Since only a whole particle can be added or removed, the nearest integer is taken and the remaining particle fraction is included at the next time step. It should be noted that although the above steps are only illustrated along the $y$-direction, multi-dimensional problems can be handled in the same way.

## 3. Results

We first consider an example of sudden-start Couette flow that is similar to the test case used by O'Connell & Thompson (1995). The fluid is confined between two parallel walls at $y = 0$ and $52.1\sigma$. The upper region $y > 15.6\sigma$ is described by the continuum NS equations and the bottom region $y < 31.3\sigma$ contains discrete Lennard–Jones atoms. The overlap region is $3\Delta y = 15.6\sigma$ wide. Periodic boundary conditions with period $52.1\sigma$ are applied in the $x$-direction. No-slip boundary conditions are imposed at the top wall, and the atomistic description of the bottom wall is chosen to produce a no-slip condition. As in O'Connell & Thompson (1995), the bottom wall consists of two (111) planes of a face-centred cubic lattice formed by molecules with the same density as the liquid. The interactions between wall and fluid molecules are described by a shifted Lennard–Jones potential with a characteristic energy $\epsilon^{wf} = 0.6\epsilon$ and length scale $\sigma^{wf} = \sigma$.

Initially, the mean fluid velocity is zero everywhere. At $t = 0$, the upper wall begins to move at a constant velocity $U = \sigma/\tau$, while the bottom wall is kept still. The analytical solution of the NS equations for these conditions was calculated assuming no-slip boundary conditions. The results were then averaged over the time intervals indicated in figure 2. At early times, only the upper region of the fluid feels the drag from the wall. At the latest times, the steady-state linear Couette profile is observed.

Symbols in figure 2 show the hybrid solution for the same time intervals. In this first test of our approach it is important to minimize statistical errors so that any systematic errors are revealed. Statistical errors are most significant over the short averaging times used at the earliest stages of flow. This noise could be reduced by increasing the thickness of the cell from the relatively small value of $\Delta z = 4.81\sigma$.

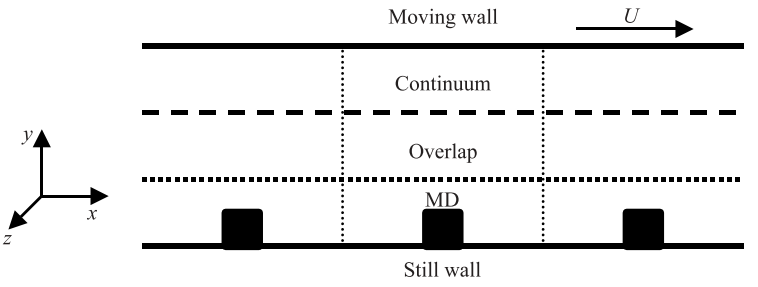


FIGURE 3. Schematic of the simulation of the channel flow with rough bottom wall by the hybrid method.

Instead we ran ten realizations of the same system in parallel on a linux cluster and averaged the results to obtain the points in figure 2. The excellent agreement of the velocity profiles from the hybrid and continuum solutions in figure 2 demonstrates that the hybrid method provides a good description of momentum coupling at the MD–continuum interface. Note also that the discrete and continuum portions of the hybrid solution track closely in the overlap region.

To test the method on a system with particle flux at the MD–continuum interface, we examined channel flow past the rough wall shown in figure 3. The rough bottom wall is modelled by two (111) planes with additional square bulges of side length $5.21\sigma$. Since the problem is periodic, only the single period demarcated by the two vertical dotted lines in figure 3 is actually simulated. The simulation domain in the $(x, y)$-plane is $46.9\sigma \times 46.9\sigma$. As above, the hybrid simulation uses continuum equations for $y > 15.6\sigma$ and MD simulations for $y < 31.3\sigma$. The continuum region is divided into $n_x \times n_y = 9 \times 6$ cells for numerical calculations. The MD region is also divided into $9 \times 6$ cells to obtain averaged velocities. Full MD and full continuum simulations with finer grids of $36 \times 36$ cells were performed for the same geometry to provide bases for comparison. The continuum simulation requires boundary conditions at the wall. Given the success of the no-slip condition for sudden-start Couette flow with a flat wall, we have assumed the no-slip velocity condition applies along the entire surface of the rough wall.

As above, the upper wall was translated at $U = \sigma/\tau$. Although this velocity is quite fast compared to typical experiments ($\sim 100\,\mathrm{m\,s^{-1}}$), previous simulations show that the response remains Newtonian and the Reynolds number is small in systems of the size used here (Thompson & Troian 1997; Koplik & Banavar 1995*a*). Both hybrid and MD simulations were run for $4000\tau$ to achieve a steady-state flow. They were then averaged over an additional $4000\tau$ and over ten (MD) or twenty (hybrid) independent runs made in parallel. Statistical variations between individual MD simulations are constant over the simulation volume. They are equivalent to variations between runs in the MD portion of hybrid simulations, while variations in the continuum portion of hybrid simulations are smaller because there is no thermal noise in these regions.

Figure 4(*a*) shows that streamlines from the hybrid method and the full MD simulation are in excellent agreement. This demonstrates that the hybrid method correctly describes both mass and momentum flux at the MD–continuum interface. Figure 4(*b*) compares the streamlines for the hybrid and the pure continuum simulation. The difference is much larger than that in figure 4(*a*), implying that the continuum description, consisting of the Navier–Stokes equations and non-slip boundary conditions, does not capture the relevant physics. As mentioned earlier, the

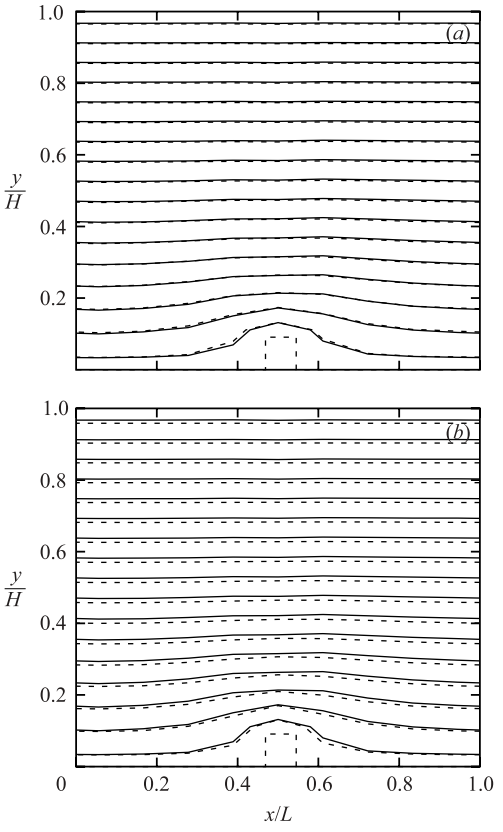


FIGURE 4. The streamlines for channel flow with a rough bottom wall. The square in the middle of the bottom wall shows the location of the bulge in the surface. In (*a*) the solid line is for the hybrid solution and the dashed line for the full atomistic solution. In (*b*) the solid line is for the hybrid solution and the dashed line for the full continuum solution.

parameters in our MD simulation were chosen so that flat walls satisfied the no-slip boundary condition. However, the complex molecular structure near the bulges seems to change the local velocity boundary conditions in a way that ultimately affects the entire flow field. Resolving this discrepancy using the Navier–Stokes equation with complex and spatially varying slip boundary conditions (Thompson & Troian 1997; Karniadakis & Beskok 2001) is in principle possible. However, the hybrid method captures these boundary conditions naturally without parameterization. In fact, it could be used to provide boundary conditions for other continuum simulations. This approach might be desirable if there were a large separation of time scales between the MD and continuum solutions.

The flow normal to the overlap region is examined directly in figure 5. Here the vertical velocity $u_y$ is plotted as a function of $y$ for each of the nine columns of bins along the $x$-direction. The statistical uncertainties for the hybrid and MD simulations are roughly $0.003\sigma/\tau$. Fluctuations of this order are expected given that thermal velocities are of order 1 and results are averaged over about 100 particles in each bin and about $10^4$ velocity auto-correlation times. We conclude that the hybrid and MD results are in excellent agreement within the statistical fluctuations. Note that there is significant flux between MD and continuum regions that is positive for some $x$

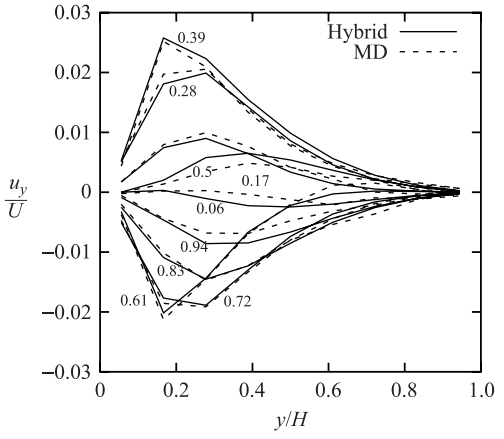


FIGURE 5. Normalized vertical velocity $u_y/U$ as a function of $y/H$ for bins centred on the indicated values of $x/L$. Solid and dashed lines are for the hybrid and MD simulations, respectively. Statistical errors in both are about $0.003\sigma/\tau$.

and negative at others. The hybrid method allows this flux to occur in a way that is statistically equivalent to the full MD solution.

## 4. Summary and conclusions

We have developed a hybrid numerical method for calculating flows in micro- or nano-scale geometries. MD simulations are used in interfacial regions where the discreteness of the fluid is important and the Navier–Stokes equations are solved in regions where a continuum description is accurate. The two descriptions are coupled by imposing continuity of fluxes at the boundaries of an overlap region. The mean particle velocities provide boundary conditions for the NS solution at one side of the overlap region (P → C in figure 1). A constrained dynamics algorithm forces the instantaneous mean particle velocity to equal the continuum solution at the other boundary (C → P in figure 1). Flux across the overlap region is maintained by adding or removing a number of particles that is consistent with the continuum flux.

Simulations of sudden-start Couette flow and flow with a nano-scale rough wall compare very well with exact solutions and full MD simulation results. This demonstrates the potential of our method for addressing complex geometries and boundary conditions. In particular, our hybrid simulation of nano-scale roughness reveals a change in boundary conditions on the bump that influences the velocity field throughout the system.

The computational efficiency of the hybrid code relative to pure MD simulations is roughly the ratio of the total volume to the portion treated atomistically. The continuum solution uses coarser time and space discretization than the MD and can be further speeded by using variable cell sizes. As a result, the computation time is almost the same as that for an MD simulation of the same size as the MD part of the hybrid algorithm. The statistical error bars for averages over the same time interval are actually smaller in the hybrid algorithm because there are no thermal fluctuations in the continuum regions. In the examples considered here, the MD region occupies about 50% of the volume and the hybrid method is less than a factor of 2 faster than an all MD simulation. However, this geometry was chosen precisely because we wanted to perform all MD simulations to validate the method. The hybrid method

can be applied to channels that are many times wider without significant increase in computation, while the MD calculations would scale linearly with system size. We are currently completing a study of the corner singularity in driven cavity flow where a full MD simulation would require hundreds of times more particles and computation than the hybrid method (Nie, Chen & Robbins 2003).

The method described here can be extended straightforwardly to higher dimensions and in several other ways. One is to the study of multiphase flows where the fluxes of each species could be controlled using constrained dynamics. It would also be interesting to include heat flux in both MD and continuum approaches. This would require knowledge of the temperature dependent-viscosity which could be obtained in advance, or by monitoring the response of fluid in the overlap regime.

This research was supported by US National Science Foundation (NSF) Grant CMS-0103408. The simulations were performed on the Johns Hopkins University cluster computer supported by US NSF Grant CTS-0079674.

## REFERENCES

Batchelor, G. K. 1967 *An Introduction to Fluid Dynamics*. Cambridge University Press.

Dussan V., E. B. 1979 Spreading of liquids on solid-surfaces-static and dynamic contact lines. *Annu. Rev. Fluid Mech.* **11**, 371–400.

Dussan V., E. B. & Davis, S. H. 1986 Stability in systems with moving contact lines. *J. Fluid Mech.* **173**, 115–130.

Flekkoy, E. G., Wagner, G. & Feder, J. 2000 Hybrid model for combined particle and continuum dynamics. *Europhys. Lett.* **52**, 271–276.

Grest, G. S. & Kremer, K. 1986 Molecular dynamics simulation for polymers in the presence of a heat bath. *Phys. Rev.* A **33**, 3628–3631.

Hadjiconstantinou, N. G. 1999 Hybrid atomistic-continuum formulations and the moving contact-line problem. *J. Comput. Phys.* **154**, 245–265.

Hadjiconstantinou, N. G. & Patera, A. T. 1997 Heterogeneous atomistic-continuum representations for dense fluid systems. *Intl J. Mod. Phys.* C **8**, 967–976.

Ho, C. M. & Tai, Y. C. 1998 Micro-electro-mechanical-systems(MEMS) and fluid flows. *Annu. Rev. Fluid Mech.* **30**, 579–612.

Huh, C. & Scriven, L. 1971 Hydrodynamic model of steady movement of a solid/liquid/fluid contact line. *J. Colloid Interface Sci.* **35**, 85–101.

Karniadakis, G. E. & Beskok, A. 2001 *Micro Flow*. Springer.

Koplik, J. & Banavar, J. R. 1995*a* Continuum deductions from molecular hydrodynamics. *Annu. Rev. Fluid Mech.* **27**, 257–292.

Koplik, J. & Banavar, J. R. 1995*b* Corner flow in the sliding plate problem. *Phys. Fluids* **7**, 3118–3125.

Koplik, J., Banavar, J. R. & Willemsen, J. F. 1988 Molecular dynamics of Poiseuille flow and moving contact lines. *Phys. Rev. Lett.* **28**, 1282–1285.

Nie, X. B., Chen, S. Y. & Robbins, M. O. 2003 Hybrid simulation of micro-cavity flow. *Phys. Fluids* (to be submitted).

O'Connell, S. T. & Thompson, P. A. 1995 Molecular dynamics-continuum hybrid computations: A tool for studying complex fluid flows. *Phys. Rev.* E **52**, R5792–5795.

Peyret, R. & Taylor, T. D. 1983 *Computational Methods for Fluid Flow*. Springer.

Saletan, E. J. & Cromer, A. H. 1971 *Theoretical Mechanics*, pp. 125–131. John Wiley & Sons.

Thompson, P. A. & Robbins, M. O. 1989 Simulations of contact-line motion: slip and the dynamic contact angle. *Phys. Rev. Lett.* **63**, 766–769.

Thompson, P. A. & Troian, S. M. 1997 A general boundary condition for liquid flow at solid surfaces. *Nature* **389**, 360–362.